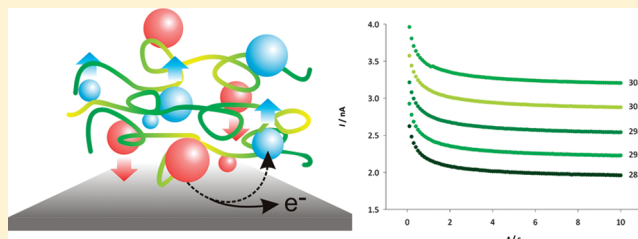


Polyazetidine-Coated Microelectrodes: Electrochemical and Diffusion Characterization of Different Redox Substrates

Massimo Di Fusco,^{†,‡} Gabriele Favero,[†] and Franco Mazzei^{*,†}[†]Dipartimento di Chimica e Tecnologie del Farmaco and [‡]Dipartimento di Chimica, Sapienza Università di Roma, Piazzale Aldo Moro 5, 00185 Rome, Italy

ABSTRACT: The present paper reports on the diffusion characteristics and electron transfer properties of a membrane obtained from polyazetidine prepolymer (PAP) consisting of repeating units of 1-(aminomethyl)-1-{2-[(6-oxohexane)amino]ethyl}-3-hydroxyazetidinium chloride studied in the presence of seven simple redox electroactive molecules: ABTS, catechol, dopamine, ferrocenecarboxylic acid, ferricyanide, ferrocyanide, and the osmium complex bis(2,2-bipyridyl)-4-aminomethylpyridine chloride hexafluorophosphate ($\text{Os}[(\text{bpy})_2 4\text{-AMP Cl}]^+$). Using water as medium, the apparent diffusion coefficients (D_{app}), the concentrations of the compounds in the membrane, and the heterogeneous rate constants (k_s) were calculated as a function of temperature, and the influence thereof on these parameters was evaluated. Even if D_{app} and k_s values in the presence of PAP are smaller than in solution, this decrease is small enough to indicate that the PAP membrane shows excellent diffusion and electron-exchange properties with respect to other commonly used membranes reported in the literature.



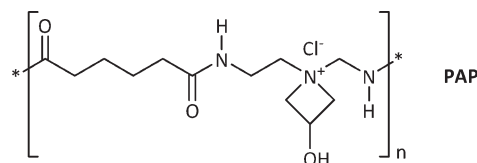
1. INTRODUCTION

The modification of electrodes with redox mediators for use as chemical sensors, transducers of biosensors, electrodes of biofuel cells, and other devices has attracted considerable attention over the past few years. One common method used for this purpose is to spread polymeric membranes over the electrode surface. Such membranes can be divided into two categories: redox polymers in which the redox active sites are included in the polymer backbone or in the side chain, and ion-exchange polymers in which the redox sites are immobilized by electrostatic attraction.^{1–11}

Much of the more recent research in this field has been focused on the ion-exchange polymeric films: the most extensively studied of these is Nafion, a perfluorinated polysulfonate material.^{12–22} Nevertheless, a problem associated with many ion-exchange polymers, including Nafion, is that they yield small diffusion coefficients for the immobilized species, specifically, a reduction of up to 4 orders of magnitude with respect to the same species free in solution. For certain applications such as electrocatalysis requiring rapid charge transfer, these small diffusion coefficients are undesirable.

In this paper, the diffusion characteristics and electron transfer properties of a membrane obtained from polyazetidine prepolymer (PAP)^{23–25} consisting of repeating units of 1-(aminomethyl)-1-{2-[(6-oxohexane)amino]ethyl}-3-hydroxyazetidinium chloride (see Scheme 1) were investigated. PAP allows both chemical and physical entrapment^{23,26} and the immobilization procedure is possible thanks to its peculiar features. PAP actually acts as a cross-linking agent as it is able to react with several different organic moieties (thiolic, oxidrilic, carboxyl, amino group), thus increasing

Scheme 1. PAP Structure



the possibility of creating chemical bonds with the enzyme and enhancing immobilization efficiency.²⁶

This polymeric membrane has been used in recent years as an enzyme-immobilizing agent in the construction of electrochemical biosensors. The efficiency of PAP as immobilizing agent for proteins, allowing them to retain their native structure and consequently also their bioelectrochemical properties, has been described in previous papers.^{23–26} However, a thorough investigation of the permeability of PAP toward redox mediators when used as an immobilizing agent in second-generation biosensor development remained to be performed. In the present work PAP was spread onto an electrode surface without the addition of other compounds to form a pure polymeric film. This film acts as a hydrogel and may thus be described as a single-phase “aqueous” matrix with excellent diffusional characteristics. Hydrogels have a number of characteristics that make them desirable electrode

Received: July 30, 2010

Revised: October 14, 2010

Published: December 30, 2010

coatings, especially for bioelectrochemical applications: high water content, biocompatibility, low interfacial tension between hydrogel surface and aqueous solution, excellent diffusion characteristics for small molecules and ions, and optical transparency.²⁷

The purpose of this work is to elucidate the effective validity of a PAP membrane as an immobilizing agent in the development of biosensors as a function of its diffusion and electron transfer characteristics in the presence of electrochemical mediators. For the purpose of PAP characterization, seven simple redox electroactive molecules were tested. These species are widely used as enzyme mediators in the development of second-generation biosensors: 2,2'-azino-bis(3-ethylbenzothiazoline-6-sulfonic acid) diammonium salt (ABTS),^{28–33} catechol,^{33–36} dopamine,^{37–40} ferrocenecarboxylic acid,⁴¹ ferricyanide,³³ ferrocyanide,^{42,43} and the osmium complex bis(2,2-bipyridyl)-4-aminomethylpyridine chloride hexafluorophosphate ($\text{Os}[(\text{bpy})_2\text{ 4-AMP Cl}]^+$).^{44–47}

2. EXPERIMENTAL SECTION

2.1. Chemicals. 2,2'-Azino-bis(3-ethylbenzothiazoline-6-sulfonic acid) diammonium salt (ABTS), catechol, dopamine, ferrocenecarboxylic acid (FcCOOH), potassium ferrocyanide (II) ($\text{K}_4[\text{Fe}(\text{CN})_6]$), potassium ferricyanide (III) ($\text{K}_3[\text{Fe}(\text{CN})_6]$), and osmium bis(2,2-bipyridyl)-4-aminomethylpyridine chloride hexafluorophosphate ($\text{Os}[(\text{bpy})_2\text{ 4-AMP Cl}]^+$) were used as received. The polymeric film employed was poly-1-(amino-methyl)-1-{2-[(6-oxysesane)amino]ethyl}-3-hydroxyazetidinium chloride (polyazetidine prepolymer (PAP), aqueous solution, 12% w/v), donated by Hercules Inc., Wilmington, DE (USA). All other chemicals were analytical grade. High purity deionized water (resistance $18.2\text{ M}\Omega\cdot\text{cm}$ at $25\text{ }^\circ\text{C}$; total organic carbon $< 10\text{ }\mu\text{g/L}$) obtained from Millipore (France) was used to prepare all the solutions.

2.2. Apparatus. Electrochemical experiments were performed using a μ -Autolab type III potentiostat (Eco Chemie, Netherlands) controlled by means of the GPES Manager program. The measurements were performed in a thermostated 10 mL glass cell with a conventional three-electrode configuration: $20 \pm 1\text{ }\mu\text{m}$ diameter (determined experimentally, vide infra) platinum microdisk encased in glass (Amel, Italy) as working electrode, Ag/AgCl (KCl saturated) (Metrohm, Switzerland, 198 mV vs NHE) as reference electrode, and a graphite rod as counter electrode. All solutions were deaerated with nitrogen before each measurement, and the supporting electrolyte was 0.1 mol/L KCl. The temperature was controlled using a Julabo F10 thermostat (temperature error $\pm 0.5\text{ }^\circ\text{C}$).

2.3. Preparation of Polyazetidine-Coated Electrodes. The platinum microdisk radius was measured before every experiment by chronoamperometric steady-state current using a $1.1\text{ mmol L}^{-1}\text{ K}_3[\text{Fe}(\text{CN})_6]$ solution in $0.1\text{ mol L}^{-1}\text{ KCl}$ (under these conditions, the diffusion coefficient of $\text{Fe}(\text{CN})_6^{3-}$ is $7.6 \times 10^{-6}\text{ cm}^2\text{ s}^{-1}$).⁴⁸ The electrode was first polished using different size alumina powders (0.3 and $0.05\text{ }\mu\text{m}$) and then ultrasonically cleaned in water for about 5 min. The PAP-coated electrode was prepared by simply depositing $3\text{ }\mu\text{L}$ of PAP solution and leaving it to dry overnight; over this period the water evaporates and the polymeric film, insoluble in water, is formed. Before measurements were performed, the PAP-coated electrode was immersed in the redox probe solution and allowed to stabilize; at the same time the potential between the reduced and oxidized forms of the compound was scanned, until a stable voltammetric profile was reached. This was done to allow the selected mediator to fill the

polymeric layer. All results are the average of five or more replicate measurements.

2.4. Measurement of Apparent Diffusion Coefficients and Standard Heterogeneous Rate Constants. Apparent diffusion coefficients were obtained by means of potential-step chronoamperometry performed on a 1 mmol L^{-1} aqueous solution of the selected compound in the presence of $0.1\text{ mol L}^{-1}\text{ KCl}$ as supporting electrolyte. The experiments were performed using a sampling time of 0.1 s. The system was pretreated by maintaining the potential at a point corresponding to the passage of zero faradic current for 10 s, after which the experimental transients were obtained by stepping to a potential value greater in absolute value with respect to the reduction or oxidization peak potential after the application of the potential step, and the current was measured for 50 s. After 10 s the current normally reaches the steady state in any case. Heterogeneous rate constants were obtained under the same experimental conditions using steady-state voltammetry at a scan rate of 5 mV s^{-1} .

3. RESULTS AND DISCUSSION

3.1. Theoretical Background. The major problem to be addressed in the chronoamperometric measurement of the diffusion coefficient using a membrane coated electrode is the unknown analyte concentration in the hydrogel; to work around this the data needs to be treated in accordance with the normalized Cottrell equation.⁴⁹ The latter consists of a rearrangement of the Cottrell equation (1) describing the chronoamperometric response of an electroactive species at a microdisk electrode:^{50,51}

$$I = (\pi^{1/2}nFD^{1/2}Cr^2)/t^{1/2} + 4nFDCr \quad (1)$$

where n is the number of electrons exchanged in the redox reaction, F is Faraday's constant, D is the diffusion coefficient, C is the analyte concentration, t is the time elapsing after the application of an appropriate potential step, and r is the radius of the microdisk electrode. Equation 1 contains both a time-independent term and a time-dependent term, with the time-independent term representing the steady-state behavior 2:

$$I_d = 4nFDCr \quad (2)$$

With short experimental times, the time-dependent term is larger than the time-independent one, which becomes more important as experimental time increases. However, this effect is more evident using a microdisk electrode. Indeed, in this case, the time-dependent Cottrellian behavior of the current response becomes negligible already a few seconds after the application of the potential step;⁵² after this short time, the time-independent term actually becomes predominant and the faradic current generated at the microelectrode surface can be described by eq 2. Normalization of a chronoamperometric response I (in eq 1) by dividing the entire current–time curve by the steady-state current I_d leads to eq 3 (normalized Cottrell equation):

$$I/I_d = (\pi^{1/2}r)/(4D^{1/2}t^{1/2}) + 1 \quad (3)$$

The plot of I/I_d vs $t^{-1/2}$ has the form of a straight line with an intercept equal to unity and a slope $S = (\pi^{1/2}r)/(4D^{1/2})$, from which it is possible to evaluate D if the radius r is known.

While potential-step chronoamperometry allows a simple evaluation of the diffusion properties, scan voltammetry can be used to investigate the efficiency of heterogeneous electron transfer. Because of the steady-state nature of the diffusion layer

at a microdisk electrode, a sigmoidal voltammogram should be obtained at a slow scan rate.⁵³ Under these conditions, the half-wave potential $E_{1/2}$ can be obtained from the following equation:

$$E = E_{1/2} + (RT/nF) \ln[I/(I_d - I)] \quad (4)$$

where all the symbols have their usual meanings and I_d is the current expressed by eq 2. $E_{1/2}$ can be easily extrapolated from a plot of E vs $\ln[I/(I_d - I)]$, and this value corresponds to the value of $E^{\circ'}$ if we assume that the diffusion coefficients of the reduced and oxidized forms are the same.

The equation for the voltammetric response of such a quasi-reversible redox reaction under steady-state conditions at a microdisk electrode was proposed by Galus et al.:⁵⁴

$$\frac{(4D/\pi k_s r) \exp[-(1 - \alpha)nf(E - E^{\circ'})]}{[(I_d - I)/I] - [(I_d - I^r)/I^r]} \quad (5)$$

where k_s is the standard heterogeneous rate constant, α is the transfer coefficient of the cathodic reaction, $f = F/RT$, I_d is the steady-state current, and I^r is the calculated reversible current using eq 6.^{55,56}

$$\ln[(I_d - I^r)/I^r] = nf(E^{\circ'} - E) \quad (6)$$

The logarithmic form of eq 5 can be used to determine k_s :

$$E - E^{\circ'} = [1/(1 - \alpha)nf] \ln(4D/\pi k_s r) - [1/(1 - \alpha)nf] \ln\{[(I_d - I)/I] - [(I_d - I^r)/I^r]\} \quad (7)$$

Using eq 7, for a given value of the radius r , the first term on the right-hand side is constant. Therefore, a plot of $E - E^{\circ'}$ vs $\ln\{[(I_d - I)/I] - [(I_d - I^r)/I^r]\}$ should be linear with slope $1/(1 - \alpha)nf$ and intercept $[1/(1 - \alpha)nf] \ln(4D/\pi k_s r)$ from which the k_s value may be easily calculated, provided that r and D are known.

3.2. Determination of Apparent Diffusion Coefficient and Electron-Exchange Constant at Different Temperatures Using Naked Microelectrode. The apparent diffusion coefficients D_{app} of seven simple redox molecules at different temperatures were determined using potential-step chronoamperometry. In this case the probe concentration is known, because of the lack of the membrane, so the data were fitted (using a nonlinear fit algorithm in SigmaPlot) according to the Cottrell equation (eq 1) and the diffusion current obtained at the steady-state I_d was used to calculate D_{app} values. As a representative example, Figure 1a shows the potential-step chronoamperometry (time = 10 s) of FcCOOH in the temperature range 288–308 K. The averaged results of all compounds are listed in Table 1. As expected, an increase in the apparent diffusion coefficients is observed as the temperature increases because of the decrease in the viscosity of the solvent media. The Stokes–Einstein equation,⁵⁷ eq 8, predicts this inverse proportionality between diffusion coefficient and viscosity (η) of the solvent.

$$D = k_B T / 6\pi\eta a \quad (8)$$

where k_B is the Boltzmann constant ($1.38 \times 10^{-23} \text{ m}^2 \text{ kg s}^{-2} \text{ K}^{-1}$), T is the temperature, and a is the hydrodynamic radius. The applicability of the Stokes–Einstein relationship was evaluated and the plots of D vs η^{-1} are shown in Figure 2; the viscosity of the measuring solution was calculated according to Kestin.⁵⁸ The hydrodynamic radii of the compounds were determined and are shown in Table 2.

The heterogeneous rate constants k_s of the compounds at different temperatures were also determined using steady-state

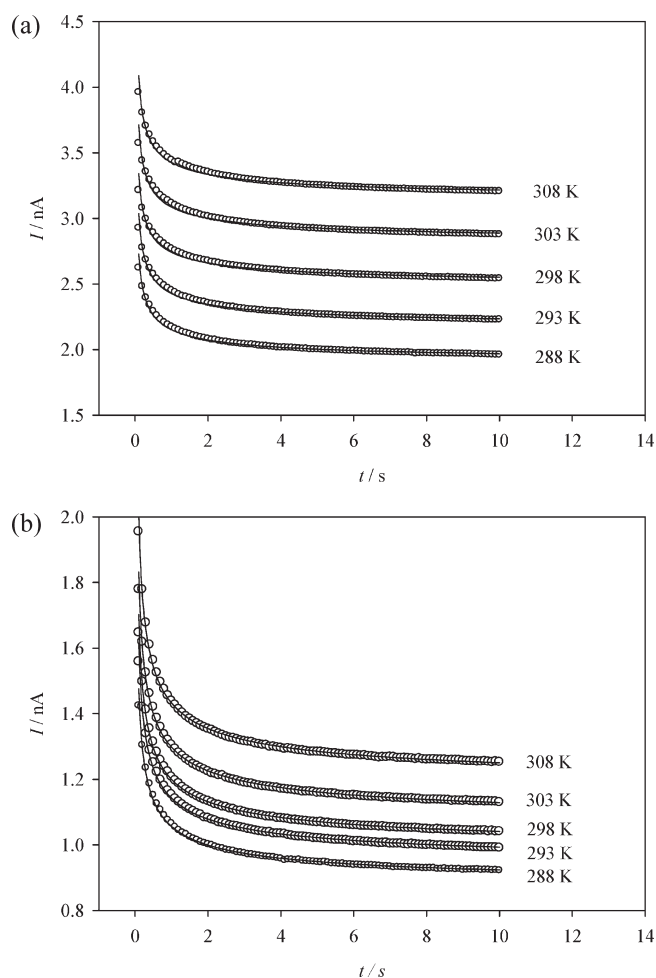


Figure 1. Potential-step chronoamperometry for 1 mmol L⁻¹ FcCOOH in 0.1 mol L⁻¹ KCl obtained at different temperatures using a platinum microelectrode in either the absence (a) or presence (b) of PAP membrane. The open circles represent the experimental points which are fitted to the Cottrell equation (solid line).

voltammetry. Figure 3a shows the steady-state voltammograms referring to the oxidation of FcCOOH over the temperature range 288–308 K. Before calculating k_s from the experimental data, it is necessary to check whether steady-state assumptions are fulfilled under the experimental conditions. To do this, the parameter p presented by Aoki et al.⁵⁹ was used:

$$p = (nFr^2\nu/RTD)^{1/2} \quad (9)$$

where ν is the scan rate and the other symbols have their usual meanings. When p is large, linear diffusion predominates and the voltammogram is peak shaped. On the other hand, when p is small, radial diffusion predominates and a sigmoidal voltammogram is obtained. In contrast, when $p < 0.33$, the voltammogram current deviates from the steady-state current by less than 5%.⁵⁹ In this work a scan rate of 5 mV s⁻¹ and a 10- μ m-radius electrode were used, so, according to eq 9, p is smaller than 1.40 assuming $D > 1.0 \times 10^{-7} \text{ cm}^2 \text{ s}^{-1}$. Under these conditions, the experimental voltammograms are acceptably close to a steady-state wave.

The data obtained from the steady-state voltammograms were fitted in accordance with eq 7, and the heterogeneous rate constants were calculated. The results obtained for the compounds

Table 1. Calculated Apparent Diffusion Coefficients and Heterogeneous Electron Transfer Constants for All Compounds Considered^a

compound	T (K)	D_{app} ($\text{cm}^2 \text{s}^{-1}$)	RSD (%)	k_s (m s^{-1})	RSD (%)
ABTS	288	2.4×10^{-6}	0.4	3.8×10^{-5}	0.5
	293	2.9×10^{-6}	0.3	4.2×10^{-5}	0.2
	298	3.4×10^{-6}	0.5	5.5×10^{-5}	0.5
	303	3.9×10^{-6}	0.2	6.7×10^{-5}	0.3
	308	4.5×10^{-6}	0.2	8.0×10^{-5}	0.2
catechol	288	1.0×10^{-5}	0.9	1.3×10^{-4}	0.7
	293	1.2×10^{-5}	0.7	1.5×10^{-4}	0.6
	298	1.3×10^{-5}	0.7	1.7×10^{-4}	0.5
	303	1.5×10^{-5}	0.6	2.0×10^{-4}	0.4
	308	1.7×10^{-5}	0.5	2.2×10^{-4}	0.4
dopamine	288	5.3×10^{-6}	0.2	7.0×10^{-5}	0.1
	293	6.1×10^{-6}	0.3	7.9×10^{-5}	0.3
	298	7.0×10^{-6}	0.1	9.1×10^{-5}	0.1
	303	7.8×10^{-6}	0.2	1.0×10^{-4}	2.7
	308	8.7×10^{-6}	0.1	1.1×10^{-4}	0.8
FcCOOH	288	4.8×10^{-6}	0.2	6.9×10^{-5}	0.1
	293	5.4×10^{-6}	0.2	7.5×10^{-5}	0.1
	298	6.2×10^{-6}	0.1	8.4×10^{-5}	0.1
	303	7.1×10^{-6}	0.3	9.3×10^{-5}	0.3
	308	7.9×10^{-6}	0.2	1.1×10^{-4}	2.4
$\text{Fe}(\text{CN})_6^{4-}$	288	4.1×10^{-6}	0.2	5.4×10^{-5}	0.2
	293	4.6×10^{-6}	0.2	6.1×10^{-5}	0.1
	298	5.2×10^{-6}	0.2	7.2×10^{-5}	0.1
	303	5.8×10^{-6}	0.3	8.4×10^{-5}	0.3
	308	6.6×10^{-6}	0.5	1.0×10^{-4}	4.5
$\text{Fe}(\text{CN})_6^{3-}$	288	6.0×10^{-6}	0.1	7.9×10^{-5}	0.1
	293	6.7×10^{-6}	0.1	8.8×10^{-5}	0.1
	298	7.5×10^{-6}	0.1	9.8×10^{-5}	0.1
	303	8.3×10^{-6}	0.1	1.1×10^{-4}	0.1
	308	9.2×10^{-6}	0.3	1.2×10^{-4}	3.0
$\text{Os}[(\text{bpy})_2 4\text{-AMP Cl}]^+$	288	1.1×10^{-6}	0.8	1.7×10^{-5}	0.5
	293	1.4×10^{-6}	0.6	2.1×10^{-5}	0.4
	298	1.8×10^{-6}	0.5	2.9×10^{-5}	0.3
	303	2.2×10^{-6}	0.4	3.4×10^{-5}	0.3
	308	2.7×10^{-6}	0.3	4.3×10^{-5}	0.2

^a With 1 mmol L⁻¹ solutions in 0.1 mol L⁻¹ KCl obtained at different temperatures using a platinum microelectrode.

are listed in Table 1. Also in this case an increase was observed in the heterogeneous rate constants with increasing temperature as result of the strict dependence of k_s on D_{app} . All the correlation plots of k_s vs D_{app} produce a straight line with $R^2 > 0.99$.

3.3. Determination of Apparent Diffusion Coefficient and Electron-Exchange Constant at Different Temperatures Using PAP-Covered Microelectrode. The apparent diffusion coefficients D_{app} of the same compounds were determined at different temperatures in the presence of a PAP membrane. Figure 1b shows the potential-step chronoamperometry of FcCOOH over the temperature range 288–308 K. Considering that in this case the unmodified Cottrell equation cannot be employed because the presence of the polymeric layer produces a variation in the concentration of the electroactive species near the electrode

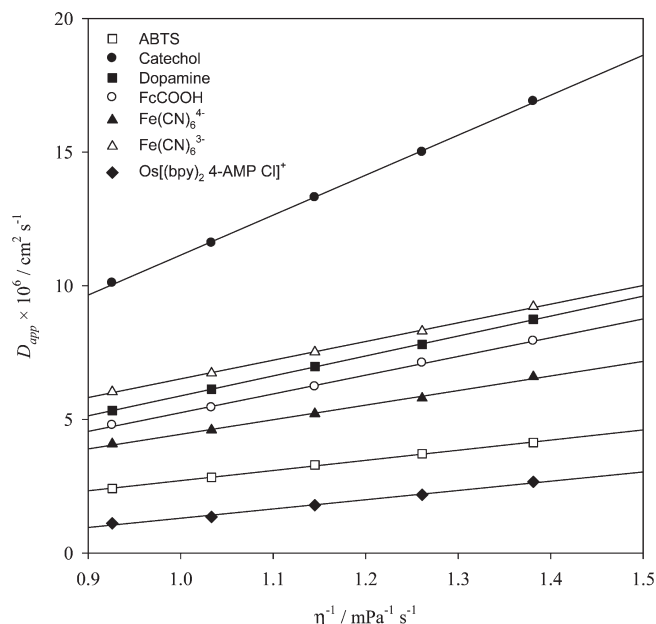


Figure 2. Calculated apparent diffusion coefficient variation vs medium viscosity, at bare electrode, for all the compounds considered: 1 mmol L⁻¹ solutions in KCl 0.1 mol L⁻¹; all other experimental conditions the same as reported in the text. The symbols represent the experimental points which are fitted to the Stokes–Einstein equation (solid lines).

Table 2. Hydrodynamic Radii for All Compounds Considered^a

compound	a (nm)
ABTS	0.674
catechol	0.171
dopamine	0.342
FcCOOH	0.364
$\text{Fe}(\text{CN})_6^{4-}$	0.467
$\text{Fe}(\text{CN})_6^{3-}$	0.365
$\text{Os}[(\text{bpy})_2 4\text{-AMP Cl}]^+$	0.738

^a With 1 mmol L⁻¹ solutions in 0.1 mol L⁻¹ KCl obtained at 298 K using a platinum microelectrode.

surface, the data were fitted according to the normalized Cottrell equation (eq 3), which allowed the diffusion coefficient to be calculated. In addition, the concentration of the compound inside the membrane was evaluated from the current I_d obtained from eq 2. The results obtained (apparent diffusion coefficients and concentrations) for all the substrates at different temperatures are listed in Table 3.

It is a known fact that in the presence of a membrane the diffusion coefficient may be affected by the electron-hopping process⁶⁰ due to the charge propagation between redox sites anchored to the film. In this case the experimental diffusion coefficient is expressed by $D = D_{phys} + D_{et}$,^{61–64} where the first term is the contribution to physical diffusion and the second is the contribution due to self-exchange electron transfer as expressed by $D_{et} = (k_{ex}\delta^2 C)/6$,⁶⁵ where k_{ex} is the electron self-exchange rate constant, δ is the distance between reaction pairs when electron exchange occurs, and C is the redox site concentration. Using as δ twice the value of the hydrodynamic radii reported in Table 2, as C the concentrations reported in Table 3, and the values of k_{ex} reported in the literature^{66–71} it is possible to

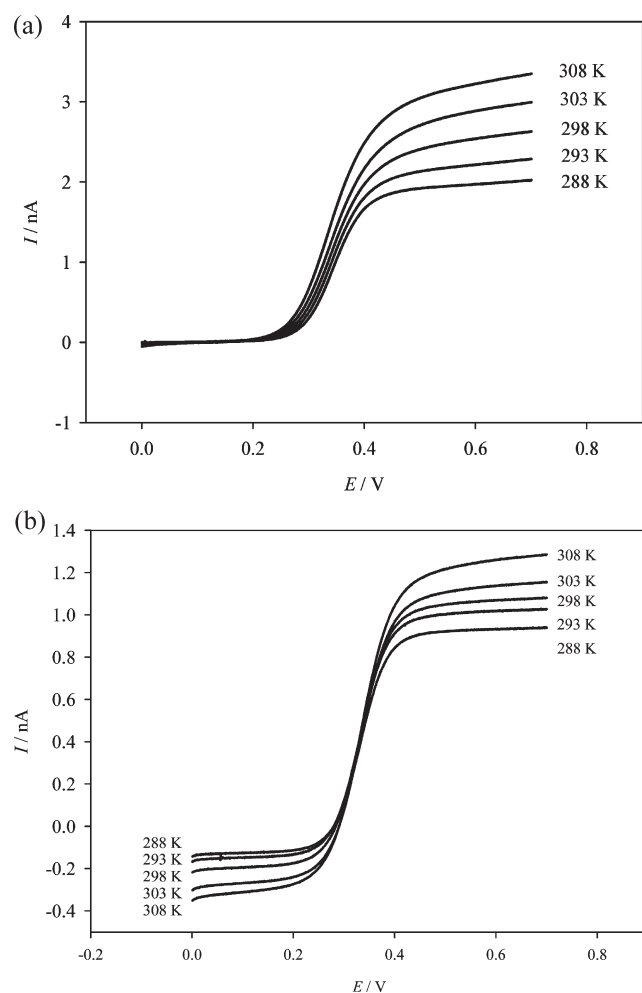


Figure 3. Steady-state voltammograms for 1 mmol L⁻¹ FcCOOH in 0.1 mol L⁻¹ KCl obtained at different temperatures using a platinum microelectrode in either the absence (a) or presence (b) of PAP membrane.

estimate the contribution of the electron hopping to the experimentally determined diffusion coefficients. Considering that the values of D_{et} (cm² s⁻¹) determined for the substrates studied were ABTS $\sim 10^{-10}$, catechol $\sim 10^{-14}$, dopamine $\sim 10^{-13}$, FcCOOH $\sim 10^{-11}$, Fe(CN)₆⁴⁻ $\sim 10^{-12}$, Fe(CN)₆³⁻ $\sim 10^{-13}$, and Os[(bpy)₂ 4-AMP Cl]⁺ $\sim 10^{-10}$, and comparing these values with those obtained experimentally and reported in Table 4, it can be assumed that electron hopping is negligible and that the D_{app} values obtained involve only physical diffusion.

From the experimental data, a decrease in D_{app} values in the presence of the coated electrode is clearly evident compared to those obtained with the bare electrode. In particular, it can be observed that on going from substrates free to diffuse from the solution to substrates forced to cross a membrane, the percent decrease of the apparent diffusion coefficient values is different for the compounds investigated and is partly related to their strength as electrolytes and their charge status. While ABTS and Fe(CN)₆³⁻ are only slightly hindered and the apparent diffusion coefficients decrease by $\sim 30\%$, the positively charged osmium complex is more strongly affected and the apparent diffusion coefficient decreases by $\sim 50\%$; on the other hand, the weak electrolytes FcCOOH, catechol, and dopamine are hindered to a much

Table 3. Calculated Apparent Diffusion Coefficients, Concentrations in Membrane, and Heterogeneous Electron Transfer Constants for All Compounds Considered^a

compound	<i>T</i> (K)	<i>D</i> _{app} (cm ² s ⁻¹)	RSD (%)	<i>C</i> (mmol L ⁻¹)	<i>k</i> _s (m s ⁻¹)	RSD (%)
ABTS	288	1.6×10^{-6}	3.9	1.84	2.8×10^{-5}	3.8
	293	2.1×10^{-6}	1.7	1.99	3.5×10^{-5}	1.8
	298	2.4×10^{-6}	1.3	1.97	4.3×10^{-5}	1.5
	303	2.8×10^{-6}	0.6	2.02	4.9×10^{-5}	0.5
	308	3.3×10^{-6}	1.9	2.01	5.8×10^{-5}	1.9
catechol	288	2.5×10^{-6}	0.4	4.12	1.0×10^{-4}	0.9
	293	2.7×10^{-6}	3.6	4.47	1.1×10^{-4}	3.3
	298	3.0×10^{-6}	2.1	4.58	1.2×10^{-4}	2.2
	303	3.2×10^{-6}	2.7	4.85	1.3×10^{-4}	2.8
	308	3.5×10^{-6}	0.3	5.06	1.4×10^{-4}	0.6
dopamine	288	1.3×10^{-6}	0.7	4.54	4.7×10^{-5}	0.8
	293	1.4×10^{-6}	1.3	4.69	5.2×10^{-5}	1.4
	298	1.5×10^{-6}	1.2	5.04	5.6×10^{-5}	1.3
	303	1.6×10^{-6}	2.8	4.94	6.6×10^{-5}	2.7
	308	1.7×10^{-6}	3.2	5.02	6.9×10^{-5}	3.1
FcCOOH	288	1.7×10^{-6}	1.1	1.76	3.2×10^{-5}	1.1
	293	1.8×10^{-6}	1.0	1.84	3.3×10^{-5}	1.1
	298	1.9×10^{-6}	1.4	1.83	3.4×10^{-5}	1.3
	303	2.1×10^{-6}	1.3	1.84	3.7×10^{-5}	1.2
	308	2.2×10^{-6}	1.2	1.95	3.9×10^{-5}	1.1
Fe(CN) ₆ ⁴⁻	288	2.3×10^{-7}	1.9	34.43	4.3×10^{-6}	1.9
	293	3.6×10^{-7}	5.7	28.41	7.1×10^{-6}	5.7
	298	5.3×10^{-7}	1.4	25.13	1.1×10^{-5}	1.6
	303	7.5×10^{-7}	3.2	22.63	1.4×10^{-5}	3.2
	308	9.8×10^{-7}	3.3	19.46	1.9×10^{-5}	3.3
Fe(CN) ₆ ³⁻	288	4.0×10^{-6}	0.7	1.90	7.0×10^{-5}	0.6
	293	4.6×10^{-6}	1.6	2.00	8.0×10^{-5}	1.6
	298	5.3×10^{-6}	1.5	2.05	9.0×10^{-5}	1.5
	303	5.9×10^{-6}	0.8	2.05	1.0×10^{-4}	0.9
	308	6.5×10^{-6}	3.2	2.09	1.1×10^{-4}	3.3
Os[(bpy) ₂ 4-AMP Cl] ⁺	288	6.9×10^{-7}	0.9	1.84	1.8×10^{-5}	1.0
	293	8.4×10^{-7}	2.3	1.79	2.2×10^{-5}	2.4
	298	9.3×10^{-7}	3.8	1.96	2.9×10^{-5}	3.7
	303	1.0×10^{-6}	0.9	2.12	3.0×10^{-5}	0.9
	308	1.1×10^{-6}	2.4	2.51	3.1×10^{-5}	2.6

^a With 1 mmol L⁻¹ solutions in 0.1 mol L⁻¹ KCl obtained at different temperatures using a platinum microelectrode in the presence of PAP membrane.

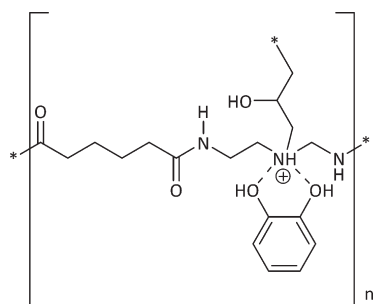
greater extent and the apparent diffusion coefficients are disrupted by ~ 70 – 80% . Finally, it is interesting to note that Fe(CN)₆⁴⁻ shows a completely different behavior with respect to the other negatively charged compounds since its D_{app} value is the most affected and decreases by $\sim 90\%$.

This clearly suggests that the polymeric structure of PAP is charged and this charge plays a crucial role in disrupting the diffusion of the selected compounds toward the electrode surface. Indeed, the membrane structure is characterized by the presence of protonatable moieties such as nitrogen atoms and amide groups that can exert a variable influence on the apparent diffusion coefficients. For instance, the positively charged polymeric structure of PAP probably causes a repulsion toward the

Table 4. Calculated Activation Energies for Diffusion and for Heterogeneous Electron Transfer for All Compounds Considered^a

compound	$E_{a,D}$ (kJ mol ⁻¹)		$E_{a,et}$ (kJ mol ⁻¹)	
	in solution	in PAP	in solution	in PAP
ABTS	19.9	21.2	23.3	25.9
catechol	19.0	12.1	19.8	13.1
dopamine	18.2	11.7	18.3	14.8
FcCOOH	18.9	7.9	15.7	7.9
Fe(CN) ₆ ⁴⁻	17.5	53.5	23.4	54.4
Fe(CN) ₆ ³⁻	15.6	18.2	15.4	16.9
Os[(bpy) ₂ 4-AMP Cl] ⁺	32.9	16.3	34.1	20.4

^aWith 1 mol L⁻¹ solutions in 0.1 mol L⁻¹ KCl using a platinum microelectrode in both the absence and presence of PAP membrane.

Scheme 2. Possible Interaction of Catechol with PAP

osmium complex, significantly reducing the corresponding apparent diffusion coefficient value. Likewise, also the substrates that are weak electrolytes could be hindered by electrostatic interactions between the protonated nitrogen atom of PAP and the $-\text{COOH}$ and $-\text{OH}$ groups present in their side chains. A possible interaction between catechol (and the same could also occur for dopamine) with PAP is shown in Scheme 2.

Although this tentative approach based on electrostatic repulsion provides some explanation of the different behaviors observed, it is far from being exhaustive: indeed, $\text{Fe}(\text{CN})_6^{4-}$ shows a different behavior with respect to the other negatively charged compounds which seems to be inexplicable, particularly in comparison with the behavior of $\text{Fe}(\text{CN})_6^{3-}$. In addition, also the variation of the concentration value in the PAP membrane for $\text{Fe}(\text{CN})_6^{4-}$ is puzzling: indeed, for the compounds considered (including $\text{Fe}(\text{CN})_6^{3-}$), the concentration in the membrane increases with increasing temperature, but $\text{Fe}(\text{CN})_6^{4-}$ not only shows an opposite trend (i.e., it decreases with increasing temperature), also the calculated values are considerably higher than all the other values. Moreover, when the membrane is examined qualitatively using a $10\times$ magnification optical microscope, although it appears flat, transparent, and hydrated after being used in the presence of the compounds considered, in the case of $\text{Fe}(\text{CN})_6^{4-}$ it becomes opaque and dry.

One explanation that could satisfactorily fit all this experimental evidence is the tendency of $\text{Fe}(\text{CN})_6^{4-}$ to form a stable ionic couple with quaternary ammonium ions while, conversely, $\text{Fe}(\text{CN})_6^{3-}$ shows no effect at all under the same conditions.⁷⁷ Compared with $\text{Fe}(\text{CN})_6^{3-}$ the apparent diffusion coefficient for $\text{Fe}(\text{CN})_6^{4-}$ is actually 10 times lower and the concentration in

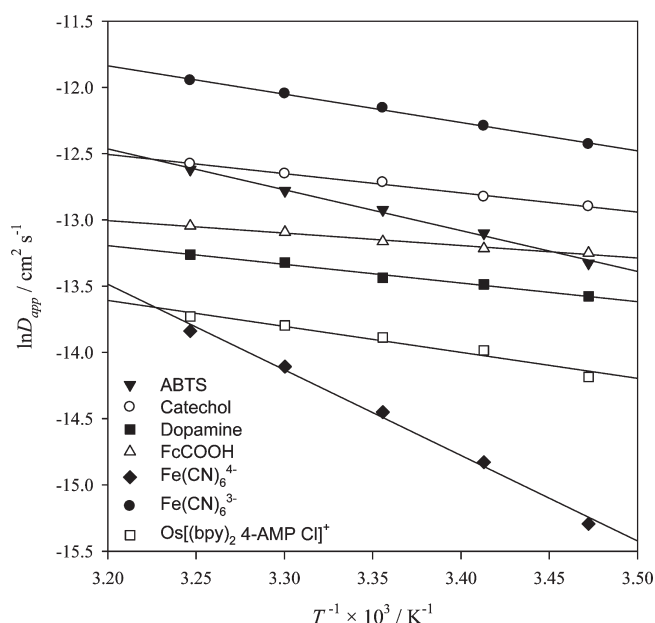


Figure 4. Calculated apparent diffusion coefficient variation vs temperature at PAP-covered electrode for all compounds considered: 1 mmol L⁻¹ solutions in KCl 0.1 mol L⁻¹; all other experimental conditions the same as reported in the text. The symbols represent the experimental points fitted to the Arrhenius equation (solid lines).

the membrane is about 10 times higher, and the latter decreases with increasing temperature depending on the thermolability of the ionic couple.

Nevertheless, even if this results in a decrease in D_{app} values in the presence of the PAP membrane compared to those measured in the absence thereof, the excellent diffusion properties of this film are enhanced, especially if they are compared with similar membranes used for the same purpose.^{72–76} Indeed, for hydrogels overlapping an electrode surface, it is quite common to reduce the diffusion coefficient to a significant extent (from a reduction of a minimum of 10-fold up to 10³-fold).^{75,76}

As already mentioned, also in the case of a membrane-covered microelectrode, an increase in the apparent diffusion coefficient values is observed with increasing temperature, even if, as expected, these calculated values are slightly lower than those determined using the bare microelectrode. To account for this behavior, two concurrent phenomena must be considered: solvent viscosity decreases with increasing temperature, thus leading to higher values of D_{app} , as already observed, and the presence of PAP membrane hinders the diffusion created, leading to lower values of D .

The heterogeneous electron transfer rate constants k_s of the compounds were also determined at different temperatures as described above. Figure 3b shows the steady-state voltammograms referring to the oxidation of FcCOOH over the temperature range 288–308 K. The results obtained for all the substrates are listed in Table 3. Also in this case an increase in the heterogeneous rate constants with increasing temperature was observed and the correlation with the apparent diffusion coefficient values was very good (plot of k_s vs D_{app} gives a straight line with $R^2 > 0.99$). Hence, also in the case of the k_s values the same trend was observed as for the apparent diffusion coefficients (i.e., related to the electrostatic properties of the compounds already considered).

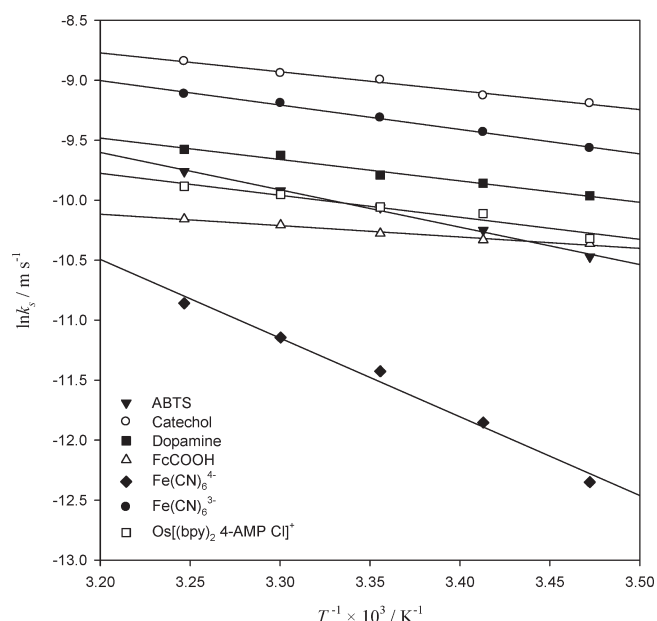


Figure 5. Calculated heterogeneous electron transfer constant variation vs temperature at PAP-covered electrode for all compounds considered: 1 mmol L⁻¹ solutions in KCl 0.1 mol L⁻¹; all other experimental conditions the same as reported in the text. The symbols represent the experimental points fitted to the Arrhenius equation (solid lines).

3.4. Calculation of Activation Energies for Diffusion and Heterogeneous Electron Exchange. The Arrhenius equations⁵⁷ of eqs 10 and 11 relate the diffusion coefficient D of electroactive species and the heterogeneous electron transfer rate constant k_s to the temperature T :

$$D = D_{\infty} \exp(-E_{a,D}/RT) \quad (10)$$

$$k_s = A \exp(-E_{a,et}/RT) \quad (11)$$

where D_{∞} is a constant corresponding to the hypothetical diffusion coefficient at infinite temperature, E_a is the activation energy of the process considered, and the other symbols have their usual meanings. Data obtained at different temperatures for both D_{app} and k_s using the microelectrode in either the presence or absence of PAP were plotted in order to calculate the corresponding activation energy. For the sake of brevity, only the plots obtained using the membrane-covered microelectrode are reported herein: in particular, Figure 4 shows the plots of $\ln D_{app}$ vs T^{-1} and Figure 5 shows the plots of $\ln k_s$ vs T^{-1} , respectively. The corresponding calculated values for the activation energies of diffusion and heterogeneous electron exchange are summarized in Table 4. As is apparent, on going from the situation in which the substrates are free to diffuse from the solution to the one in which the substrates are hindered by the presence of the PAP membrane, a negligible increase in activation energy is observed for the both ABTS and $\text{Fe}(\text{CN})_6^{3-}$ while a decrease by half is detected for the others, except $\text{Fe}(\text{CN})_6^{4-}$. Again, the unexpected behavior of $\text{Fe}(\text{CN})_6^{4-}$ could be explained by taking into account the previously discussed hypothesis of the formation of an ionic couple between the complex and the membrane leading to a reduction in the mobility of the compound, as is confirmed also by the 3-fold increase in activation energy.

Nevertheless, the calculated values of activation energies for diffusion and heterogeneous electron transfer measure the effect of temperature variation on the values of D_{app} and k_s ,

respectively. It can be concluded that the presence of PAP disrupts the influence of temperature as follows: it is practically the same for ABTS and $\text{Fe}(\text{CN})_6^{3-}$, which decreased from ca. 20% to ca. 40% for catechol and dopamine, decreased by about half for FcCOOH and osmium complex, and was 3 times greater for $\text{Fe}(\text{CN})_6^{4-}$.

4. CONCLUSIONS

The properties of PAP membrane toward the diffusion and electron exchange of a series of seven simple redox molecules was studied by steady-state voltammetry and potential-step chronoamperometry. Apparent diffusion coefficients, concentrations of the compounds in the membrane, and heterogeneous rate constants have been reported as a function of temperature. Also, the influence of temperature on the above parameters was evaluated by calculating the activation energies from the relative Arrhenius equations. Even if the D_{app} and k_s values in the presence of PAP are smaller than in solution, this reduction is small enough to indicate that the PAP membrane possesses excellent diffusion and electron-exchange properties with respect to other membranes that are frequently used and reported in the literature. The results indicate a very good permeability of the PAP layer to classical electrochemical mediators, except for $\text{Fe}(\text{CN})_6^{4-}$, the performance of which is probably disrupted by the formation of a relatively stable ionic couple with the polymeric structure of the hydrogel. This is of great importance in view of the use of PAP as an immobilizing agent in second-generation biosensor development.

AUTHOR INFORMATION

Corresponding Author

*Phone: +39-06-49913225. Fax: +39-06-49913133. E-mail: franco.mazzei@uniroma1.it.

ACKNOWLEDGMENT

This work was supported by the European Commission (BioMedNano-project NMP4-CT-2006-017350).

REFERENCES

- (1) Rigla, M.; Hernando, M. E.; Gomez, E. J.; Bragues, E.; Garcia-Saez, G.; Capel, I.; Pons, B.; de Leiva, A. *Diabetes Technol. Ther.* **2008**, *10*, 194–199.
- (2) Heller, A. *Annu. Rev. Biomed. Eng.* **1999**, *1*, 153–175.
- (3) Barton, C. S.; Gallaway, J.; Atanassov, P. *Chem. Rev.* **2004**, *104*, 4867–4886.
- (4) Heller, A. *Phys. Chem. Chem. Phys.* **2004**, *6*, 209–216.
- (5) Willner, I. *Biofuel. Fuel Cells* **2009**, *9*, 5.
- (6) Suwansa-Ard, S.; Kanatharan, P.; Asawatreratanakul, P.; Limsakul, C.; Wongkittisuksa, B.; Thavarungkul, P. *Biosens. Bioelectron.* **2005**, *21*, 445–454.
- (7) Tizzard, A. C.; Lloyd-Jones, G. *Biosens. Bioelectron.* **2007**, *22*, 2400–2407.
- (8) Liu, L. J.; Chen, Z. C.; Yang, S. N.; Jin, X.; Lin, X. F. *Sens. Actuators, B: Chem.* **2008**, *129*, 218–224.
- (9) Liu, Y.; Dong, S. J. *Biosens. Bioelectron.* **2007**, *23*, 593–597.
- (10) Cracknell, J. A.; Vincent, K. A.; Armstrong, F. A. *Chem. Rev.* **2008**, *108*, 2439–2461.
- (11) Ramanavicius, A.; Kausaite, A.; Ramanaviciene, A. *Biosens. Bioelectron.* **2005**, *20*, 1962–1967.
- (12) Rubinstein, I.; Bard, A. J. *J. Am. Chem. Soc.* **1980**, *102*, 6641–6642.
- (13) Buttry, D. A.; Anson, F. C. *J. Am. Chem. Soc.* **1982**, *104*, 4824–4829.
- (14) Martin, C. R. *J. Chem. Soc., Faraday Trans. 1* **1986**, *82*, 1051–1070.
- (15) Fortier, G.; Beliveau, R.; Leblond, E.; Belanger, D. *Anal. Lett.* **1990**, *23*, 1607–1619.

- (16) Pan, S.; Arnold, M. A. *Talanta* **1996**, *43*, 1157–1162.
- (17) Gogol, E. V.; Evtugyn, G. A.; Marty, J.-L.; Budnikov, H. C.; Winter, V. G. *Talanta* **2000**, *53*, 379–389.
- (18) Tsai, Y.-C.; Li, S.-C.; Chen, J.-M. *Langmuir* **2005**, *21*, 3653–3658.
- (19) Castro, S. S. L.; Mortimer, R. J.; de Oliveira, M. F.; Stradiotto, N. R. *Sensors* **2008**, *8*, 1950–1959.
- (20) Shie, J.-W.; Yogeswaran, U.; Chen, S.-M. *Talanta* **2009**, *78*, 896–902.
- (21) George, S.; Lee, H. K. *J. Phys. Chem. B* **2009**, *113*, 15445–15454.
- (22) Zain, Z. M.; O'Neill, R. D.; Lowry, J. P.; Pierce, K. W.; Tricklebank, M.; Dewa, A.; Ghani, S. A. *Biosens. Bioelectron.* **2010**, *25*, 1454–1459.
- (23) Frascioni, M.; Favero, G.; Di Fusco, M.; Mazzei, F. *Biosens. Bioelectron.* **2009**, *24*, 1424–1430.
- (24) Di Fusco, M.; Tortolini, C.; Deriu, D.; Mazzei, F. *Talanta* **2010**, *81*, 235–240.
- (25) Tortolini, C.; Di Fusco, M.; Frascioni, M.; Favero, G.; Mazzei, F. *Microchem. J.* **2010**, *96*, 301–307.
- (26) Mazzei, F.; Botrè, F.; Montilla, S.; Pilloton, R.; Podestà, E.; Botrè, C. *J. Electroanal. Chem.* **2004**, *574*, 95–100.
- (27) Ratner, B. D.; Hoffman, A. S. *Hydrogels for Medical and Related Applications*; Andrade, J. D., Ed.; ACS Symposium Series 31; American Chemical Society: Washington, DC, 1976; pp 1–36.
- (28) Potthast, A.; Rosenau, T.; Chen, C. L.; Gratzl, J. S. *J. Mol. Catal. A: Chem.* **1996**, *108*, 5–9.
- (29) Majcherczyk, A.; Johannes, C.; Hüttermann, A. *Appl. Microbiol. Biotechnol.* **1999**, *51*, 267–276.
- (30) Muheim, A.; Fiechter, A.; Harvey, P. J.; Schoemaker, H. E. *Holzforchung* **1992**, *46*, 121–126.
- (31) Solís-Oba, M.; Ugalde-Saldivar, V. M.; González, I.; Viniegra-González, G. *J. Electroanal. Chem.* **2005**, *579*, 59–66.
- (32) Branchi, B.; Galli, C.; Gentili, P. *Org. Biomol. Chem.* **2005**, *3*, 2604–2614.
- (33) Baminger, U.; Ludwig, R.; Galhaup, C.; Leitner, C.; Kulbe, K. D.; Haltrich, D. *J. Mol. Catal. B: Enzym.* **2001**, *11*, 541–550.
- (34) Solná, R.; Skládál, P. *Electroanalysis* **2005**, *17*, 2137–2146.
- (35) Haghighi, B.; Gorton, L.; Ruzgas, T.; Jönsson, L. *J. Anal. Chim. Acta* **2003**, *487*, 3–14.
- (36) Portaccio, M.; Di Martino, S.; Maiuri, P.; Durante, D.; De Luca, P.; Lepore, M.; Bencivenga, U.; Rossi, S.; De Maio, A.; Mita, D. *J. Mol. Catal. B: Enzym.* **2006**, *41*, 97–102.
- (37) Jarosz-Wilkolazka, A.; Ruzgas, T.; Gorton, L. *Talanta* **2005**, *66*, 1219–1224.
- (38) Xiang, L.; Lin, Y.; Yu, P.; Mao, L. *Electrochim. Acta* **2007**, *52*, 4144–4152.
- (39) Ferry, Y.; Leech, D. *Electroanalysis* **2005**, *17*, 113–119.
- (40) Osina, M. A.; Bogdanovskaya, V. A.; Tarasevich, M. R. *Russ. J. Electrochem.* **2003**, *39*, 407–412.
- (41) Jusoh, N.; Abdul-Aziz, A. *Proceedings of the 20th Symposium of Malaysian Chemical Engineers*; UiTM Universiti Teknologi MARA Pub: Shah Alam, Selangor Darul Ehsan, Malaysia, 2006; pp 29–34.
- (42) Liu, Y.; Liu, H.; Qian, J.; Deng, J.; Yu, T. *Electrochim. Acta* **1996**, *41*, 77–82.
- (43) Claus, H.; Faber, G.; König, H. *Appl. Microbiol. Biotechnol.* **2002**, *59*, 672–678.
- (44) Trudeau, F.; Daigle, F.; Leech, D. *Anal. Chem.* **1997**, *69*, 882–886.
- (45) Boland, S.; Foster, K.; Leech, D. *Electrochim. Acta* **2009**, *54*, 1986–1991.
- (46) Jenkins, P. A.; Boland, S.; Kavanagh, P.; Leech, D. *Bioelectrochemistry* **2009**, *76*, 162–168.
- (47) Boland, S.; Barrière, F.; Leech, D. *Langmuir* **2008**, *24*, 6351–6358.
- (48) Von Stackelberg, M. V.; Pilgram, M. Z. *Elektrochem.* **1953**, *57*, 342–350.
- (49) Denuault, G.; Mirkin, M. V.; Bard, A. J. *J. Electroanal. Chem.* **1991**, *308*, 27–38.
- (50) Bard, A. J.; Faulkner, L. R. *Electrochemical Methods: Fundamentals and Applications*, 2nd ed.; Wiley: New York, 2001.
- (51) Cottrell, F. G. Z. *Phys. Chem., Stoechiom. Verwandtschaftsl.* **1902**, *42*, 385.
- (52) Petrovic, S. C.; Hammericksen, R. H. *Electroanalysis* **2002**, *14*, 599–604.
- (53) Howell, J. O.; Wightman, R. M. *J. Phys. Chem.* **1984**, *88*, 3915–3918.
- (54) Galus, Z.; Golas, J.; Osteryoung, J. J. *Phys. Chem.* **1988**, *92*, 1103–1107.
- (55) Jun, Z.; Wang, J.; Tai, Z.; Ju, H. *J. Electroanal. Chem.* **1995**, *381*, 231–234.
- (56) Zhou, H.; Dong, S. J. *Electroanal. Chem.* **1997**, *425*, 55–59.
- (57) Compton, R. G.; Banks, C. E. *Understanding Voltammetry*; World Scientific Publishing: Singapore, 2007.
- (58) Grimes, C. E.; Kestin, J.; Khalifa, H. E. *J. Chem. Eng. Data* **1979**, *24*, 121–126.
- (59) Aoki, K.; Akimoto, K.; Tokuda, K.; Matsuda, H.; Osteryoung, J. G. *J. Electroanal. Chem.* **1984**, *171*, 219–230.
- (60) Kaufman, F. B.; Engler, E. M. *J. Am. Chem. Soc.* **1979**, *101*, 547–549.
- (61) Dahms, H. *J. Phys. Chem.* **1968**, *72*, 362–364.
- (62) Ruff, I. *Electrochim. Acta* **1970**, *15*, 1059.
- (63) Ruff, I.; Friedrich, V. J. *J. Phys. Chem.* **1971**, *75*, 3297–3302.
- (64) Ruff, I.; Friedrich, V. J.; Demeter, K.; Csillag, K. *J. Phys. Chem.* **1971**, *75*, 3303–3309.
- (65) Watanabe, M.; Wooster, T. T.; Murray, R. W. *J. Phys. Chem.* **1991**, *95*, 4573–4579.
- (66) Scott, S. L.; Chen, W. J.; Bakac, A.; Espenson, J. H. *J. Phys. Chem.* **1993**, *97*, 6710–6714.
- (67) Steenken, S.; Neta, P. *J. Phys. Chem.* **1979**, *83*, 1134–1137; dopamine to a good approximation was considered to have the same k_{ex} as catechol.
- (68) Nielson, R. M.; McManis, G. E.; Safford, L. K.; Weaver, M. J. *J. Phys. Chem.* **1989**, *93*, 2152–2157; k_{ex} of FcCOOH was approximated to the known value of k_{ex} of ferrocene, taking into account that the ferrocene derivatives should have similar values of λ_{ex} (see ref 69).
- (69) Baciocchi, E.; Bietti, M.; Di Fusco, M.; Lanzalunga, O. *J. Org. Chem.* **2007**, *72*, 8748–8754.
- (70) Khoshtariya, D. E.; Meusinger, R.; Billing, R. *J. Phys. Chem.* **1995**, *99*, 3592–3597.
- (71) Zakeeruddin, S. M.; Fraser, D. M.; Nazeeruddin, M. K.; Gratzel, M. *J. Electroanal. Chem.* **1992**, *337*, 253–283.
- (72) Bodor, S.; Zook, J. M.; Lindner, E.; Toth, K.; Gyurcsanyi, R. E. *Analyst (Cambridge, U.K.)* **2008**, *133*, 635–642.
- (73) Yin, Y.; Zhang, H.; Nishinari, K. *J. Phys. Chem. B* **2007**, *111*, 1590–1596.
- (74) Yamauchi, A.; Mishima, Y.; El Sayed, A. M.; Sugito, Y. *J. Membr. Sci.* **2006**, *283*, 386–392.
- (75) Henry, R. M.; Ford, C. A.; Pyati, R. *Solid State Ionics* **2002**, *146*, 151–156.
- (76) Crumbliss, A. L.; Perine, S. C.; Edwards, A. K.; Rillema, D. P. *J. Phys. Chem.* **1992**, *96*, 1388–1394.
- (77) Cohen, S. R.; Plane, R. A. *J. Phys. Chem.* **1957**, *61*, 1096–1100.